

Robust Defense Strategy for Gas-Electric Systems Against Malicious Attacks

Cheng Wang, Wei Wei, *Member, IEEE*, Jianhui Wang, *Senior Member, IEEE*, Feng Liu, *Member, IEEE*, Feng Qiu, *Member, IEEE*, Carlos M. Correa-Posada, *Student Member, IEEE*, Shengwei Mei, *Fellow, IEEE*

Abstract—This paper proposes a methodology to identify and protect vulnerable components of connected gas and electric infrastructures from malicious attacks, and to guarantee a resilient operation by deploying valid corrective actions (while accounting for the interdependency of gas pipeline network and power transmission network). The proposed mathematical formulation reduces to a tri-level optimization problem, where the lower level is a multiperiod economic dispatch of the gas-electric system, the middle level distinguishes the most threatening attack on the coupled physical infrastructures, and the upper level provides optimal preventive decisions to reinforce the vulnerable components and increase the system resilience. By reformulating the lower level problem as a mixed integer linear programming (MILP), a nested column-and-constraint generation (C&CG) algorithm is developed to solve the min-max-min model. Case studies on two test systems demonstrate the effectiveness and efficiency of the proposed methodology.

Index Terms—natural gas system, power system, interdependency, tri-level optimization, vulnerability.

NOMENCLATURE

Most of the symbols and notations used throughout this paper are defined below for quick reference. Others are defined following their first appearances, as needed.

A. Sets and Indices

$t \in T$	Time periods
$g \in G$	Traditional units
$n \in N$	Gas-fired units
$i \in I$	Power grid nodes
$l \in L$	Power grid lines
$d \in D$	Power grid loads
$w \in W$	Gas wells
$s \in S$	Gas storage tanks
$c \in C$	Gas compressors
$j \in J$	Gas network nodes
$y \in Y$	Gas network lines
$e \in E$	Gas loads

This work is supported by the National Natural Science Foundation of China (51321005). The work of J. Wang and F. Qiu is sponsored by the U. S. Department of Energy. (*Correspond to: Wei Wei*)

C. Wang, W. Wei, F. Liu, and S. Mei are with Department of Electrical Engineering, Tsinghua University, 100084 Beijing, China. (c-w12@mails.tsinghua.edu.cn; wei-wei04@mails.tsinghua.edu.cn).

J. Wang and F. Qiu are with Argonne National Laboratory, Argonne, IL 60439, USA (jianhui.wang@anl.gov; fqiu@anl.gov).

C. M. Correa-Posada is with the Colombian System Operator XM, Medellin, Colombia (cmcorrea@xm.com.co).

B. Parameters

X	Defense budget
A	Attack budget
P_g^{min} / P_g^{max}	Output range of traditional units
P_n^{min} / P_n^{max}	Output range of gas-fired units
R_+^g / R_-^g	Ramp up/down limits of traditional units
R_+^n / R_-^n	Ramp up/down limits of gas-fired units
F_l	Power transmission line capacity
p_{dt}	Power load demand
π_l	Reactance of transmission line
$f_g(\cdot)$	Generation cost of traditional units
Q_d	Not-served load cost coefficient
u_{gt}, u_{nt}	Generator status
τ_j^u, τ_j^l	Gas pressure range
$q_{s,max}^{in}, q_{s,max}^{out}$	Maximum gas storage in/out range
r_s^u, r_s^l	Maximum/minimum gas storage level
β_n	Gas-electric conversion factor
γ_c	Compression factor of the compressor
ϕ_y	Weymouth equation coefficient
Q_w, Q_e, Q_s	Gas production/not-served/storage cost
q_{et}	Gas load
$Temp$	Temperature
Z_y	Compression factor of the pipeline
$Line_y$	Length of the pipeline
R_y	Diameter
ρ_0	Gas density in standard condition
μ	Specific gas constant
F_y	Pipeline friction coefficient
λ	Unit transformation constant

C. Variables

x_l	Defend resources of power transmission line
x_y, x_n, x_c	Defend resources of pipeline/con-line/com-line
a_l	Attack resources of power transmission line
a_y, a_n, a_c	Attack resources of pipeline/con-line/com-line
z_{gt} / z_{nt}	Generator cut-out/connection decision
p_{gt}, p_{nt}	Generation output
Δp_{dt}	Not-served power load
θ	Phase angle
p_{flt}	Power flow
q_{wt}	Gas well output
$q_{st}^{in} / q_{st}^{out}$	Gas storage in/out rate
r_{st}	Stored gas amount
q_{yt}, q_{ct}	Gas flow
v_{jt}	Gas pressure square
Δq_{et}	Not-served gas

I. INTRODUCTION

OVER the past decade, technology breakthroughs in horizontal drilling and hydraulic fracturing have fostered the production of natural gas trapped within shale rock formations, and natural gas prices have dropped sharply, creating a growing demand for this energy resource from the electric power industry. However, the growing interdependency between the pipeline network for natural gas and power systems through gas-fired power plants also imposes remarkable challenges for the coordinated planning and operation of both physical systems [1], which has been well studied in [2]–[4].

Due to its fast response, gas-fired units are usually managed to compensate, in real-time, the discrepancy between generation and load, especially in the presence of a high penetration of renewable energies. Recently, many interesting and inspiring works have been found. A method for stochastic unit commitment is proposed in [5] for jointly operating natural gas and power systems to mitigate the variability of wind generation. A look-ahead robust scheduling model of a gas-electric system, which takes the natural gas congestion into account, is investigated in [6]. The importance of modeling the infrastructure for gas delivery in a power system operation with high wind power penetrations is studied in [7]. To absorb excessive wind power, power-to-gas (P2G) technology is comprehensively discussed in [8] and [9], which allows a bi-directional interchange of energy, and further enhances the interdependency between natural gas systems and power systems.

Outside the normal operating condition, there could be deliberate sabotage against these critical infrastructures, which might cause catastrophic contingencies such as line tripping and generator outage. The vulnerability assessment for power systems alone is extensively studied in [10]–[14]. The resilience of natural gas networks during conflicts, crises, and disruptions were studied in [15]. In [16], a bilevel linear programming model is proposed to assess the vulnerability of microgrids with multiple energy carriers and then deploy redispatch after deliberate interdictions. In [13], a tri-level programming model is devised to determine the optimal defensive strategy for protecting critical power system components before an attack. A column-and-constraint generation (C&CG) method is suggested to solve the tri-level optimization model. It becomes apparent that deploying preventive defenses could be one of the most effective ways to enhance system reliability.

In fact, from a robust optimization perspective, both nodal power injection uncertainty and unexpected equipment failure can be regarded and modeled as some kind of attack, yielding a min-max-min problem, such as the robust unit commitment problem considered in [17]. This paper proposes a systematic methodology to identify the most threatening attacks against the gas-electric system while taking both preventive and corrective actions into account. The contributions are twofold:

1) A defender-attacker-defender (D-A-D) formulation for protecting critical components of the interconnected gas-electric system. The decision variables of the upper level and lower level are the preventive and corrective actions of the defender, say, the system operator. They strive to minimize the

total operation cost in the worst-case disruption, including the penalty of not-served power and gas. The decision variables of the middle level are controlled by a virtual attacker, who seeks the most disruptive sabotage against the system. Our formulation is different from existing ones in the following ways. Compared with [16], we incorporate the model of reinforcing system components before the attack, which is important for enhancing system resilience. In other words, the formulation in [16] yields an attacker-defender (A-D) model with a bilevel structure. Compared with [13], we model the operation of a natural gas system, which gives rise to a nonlinear and non-convex optimization problem due to the presence of Weymouth equation. Moreover, we consider a multiperiod economic dispatch in the lower level, which captures the subsequent effects of the attack over time; we allow the generators to cut in and out and prohibit over generation after the attack occurs, providing additional flexibility for corrective control. However, this introduces binary variables in the lower level, making the problem much more challenging to solve. This leads to the second contribution.

2) A nested C&CG algorithm for solving the D-A-D model. The linear min-max-min program in [13] can be solved by the C&CG algorithm proposed in [18]. However, the non-convexity introduced by the gas pressure equation and the discontinuity brought by committing generation units prevents dualizing the lower level problem and complicates the computation. The method in [16] ignores the discontinuity from committing generators and uses a linear approximation of the Weymouth equation, so as to build a linear lower level problem. In the proposed method, the Weymouth equation is first replaced by its piecewise linear approximation with mixed integer linear form [19], yielding a mixed integer linear programming (MILP) lower level, then the nested C&CG algorithm proposed in [20] is applied to solve the D-A-D model with discrete recourse decisions. Due to the modeling capacity of MILP, our method is versatile enough to take into account a broader class of corrective actions in response to the attack.

Although the proposed model currently does not consider the uncertainty of renewable generation, there is no practical difficulty in accounting for it by using a method similar to [17]. Specifically, one can derive the identical compact model to Section II.C if a polyhedral uncertainty set is adopted. The remaining part of the paper is organized as follows. Section II presents the mathematical formulation. Section III derives the solution methodology. Section IV provides numerical results on two test systems to validate the proposed model and algorithm. Finally, Section V presents the conclusion.

II. PROBLEM FORMULATION

A. Defender-Attacker-Defender Formulation

To evaluate vulnerable components of a networked system, it is natural to introduce a virtual attacker who seeks the most serious disruption to a series of system components, while the defender can take measures before and after the attack that enhance the vulnerable equipment or respond to an attack by redispatching available resources, leading to a tri-level D-A-D model. Before the mathematical formulation is presented,

some prerequisite assumptions and simplifications to facilitate model formulation are stated as follows:

1) For modeling the gas system, we assume: i. the gas system operates in steady-state, which means the line pack (and thus the pressure dynamics of gas flow) are ignored. For the dynamic gas system modeling, refer to [19]; ii. the valve of the pipeline stays open unless it is attacked; iii. we adopt the simplified compressor model in [21], for detailed modeling of the compressor, please refer to [2].

2) For modeling the commitment of generators, we assume all generators are fast-response units, and that the cut-out/connection process is instantly completed without delay. This assumption is usually valid for gas-fired units. However, our modeling paradigm has no difficulty in modeling units that are not fast-response, as the minimal on-off time requirements can be formulated as mixed integer linear constraints.

3) For the rules of the defense and attack, we assume: i. one component fails completely if it is not defended and is attacked; ii. the component will be fully functional if it is defended, regardless of being attacked or not.

In the D-A-D model, the defender must find and deploy the optimal protection strategy in the first stage (upper level); then the attacker calculates the optimal attack strategy according to the deployment of defense resources and attacks the system in the second stage (middle level); after that, the defender responds to the attack to minimize the cost and damage, leading to the following tri-level formulation

$$Obj_{upper} = \min_{\Phi_{up}} F_{OC} \quad (1)$$

$$s.t. \quad \sum_l x_l + \sum_y x_y + \sum_n x_n + \sum_c x_c \leq X \quad (2)$$

$$x_l, x_y, x_n, x_c \in \{0, 1\} \quad (3)$$

$$Obj_{middle} = \max_{\Phi_{mid}} F_{OC} \quad (4)$$

$$s.t. \quad \sum_l a_l + \sum_y a_y + \sum_n a_n + \sum_c a_c \leq A \quad (5)$$

$$a_l, a_y, a_n, a_c \in \{0, 1\} \quad (6)$$

$$Obj_{lower} = \min_{\Phi_{low}} F_{OC} \quad (7)$$

$$s.t. \quad b_{\{\cdot\}} = 1 - a_{\{\cdot\}} + a_{\{\cdot\}} x_{\{\cdot\}}, \quad \{\cdot\} = \{l, n, y, c\} \quad (8)$$

$$z_{gt} u_{gt} P_{min}^g \leq p_{gt} \leq z_{gt} u_{gt} P_{max}^g \quad (9)$$

$$z_{nt} b_n u_{nt} P_{min}^n \leq p_{nt} \leq z_{nt} b_n u_{nt} P_{max}^n \quad (10)$$

$$p_{g,t+1} - p_{gt} \leq z_{gt} u_{gt} R_+^g + (1 - z_{g,t+1} u_{g,t+1}) P_{max}^g \quad (11)$$

$$p_{gt} - p_{g,t+1} \leq z_{g,t+1} u_{g,t+1} R_-^g + (1 - z_{gt} u_{gt}) P_{max}^g \quad (12)$$

$$p_{n,t+1} - p_{nt} \leq z_{nt} u_{nt} R_+^n + (1 - z_{n,t+1} u_{n,t+1}) P_{max}^n \quad (13)$$

$$p_{nt} - p_{n,t+1} \leq z_{n,t+1} u_{n,t+1} R_-^n + (1 - z_{nt} u_{nt}) P_{max}^n \quad (14)$$

$$0 \leq \Delta p_{dt} \leq p_{dt} \quad (15)$$

$$-\pi \leq \theta_{it} \leq \pi \quad (16)$$

$$\begin{aligned} & \sum_{\{\cdot\} \in \phi_{\{\cdot\}}(i)} p_{\{\cdot\}t} + \sum_{l \in \phi_{O_2}(i)} p_{flt} - \sum_{l \in \phi_{O_1}(i)} p_{flt} - \dots \\ & - \sum_{d \in \phi_d(i)} (p_{dt} - \Delta p_{dt}) = 0, \quad \{\cdot\} = \{g, n\} \end{aligned} \quad (17)$$

$$-F_l \leq p_{flt} \leq F_l \quad (18)$$

$$\pi_l p_{flt} = b_l (\theta_{i_1 t} - \theta_{i_2 t}), \quad i_1 \in O_1(l), i_2 \in O_2(l) \quad (19)$$

$$q_w^l \leq q_{wt} \leq q_w^u \quad (20)$$

$$r_s^l \leq r_{st} = r_{s,t-1} + q_{st}^{in} - q_{st}^{out} \leq r_s^u \quad (21)$$

$$0 \leq q_{st}^{in} \leq q_{s,max}^{in} \quad (22)$$

$$0 \leq q_{st}^{out} \leq q_{s,max}^{out} \quad (23)$$

$$(\tau_j^l)^2 \leq v_{jt} \leq (\tau_j^u)^2 \quad (24)$$

$$\begin{aligned} & \sum_{s \in \phi_s(j)} (q_{st}^{out} - q_{st}^{in}) - \sum_{e \in \phi_e(j)} (q_{et} - \Delta q_{et}) + \\ & + \sum_{w \in \phi_w(j)} q_{wt} - \sum_{n \in \phi_n(j)} p_{nt} / \beta_n = \sum_{\{\cdot\} \in \phi_{\{\cdot\}}(j)} q_{\{\cdot\}t} \end{aligned} \quad (25)$$

$$\sum_{\{\cdot\} \in \phi_{\{\cdot\}}(j)} q_{\{\cdot\}t}, \quad \{\cdot\} = \{c, y\} \quad (26)$$

$$0 \leq \Delta q_{et} \leq q_{et} \quad (26)$$

$$q_{yt} |q_{yt}| = \phi_y b_y (v_{j_1 t} - v_{j_2 t}) \quad (27)$$

$$\phi_y = \frac{\pi^2 \lambda^2 R_y^5}{16 Line_y F_y \mu Temp Z_y \rho_0^2} \quad (28)$$

$$v_{j_2} \leq \gamma_c^2 b_c v_{j_1} + (1 - b_c) (\tau_{j_2}^u)^2, \quad j_1, j_2 \in \phi(c) \quad (29)$$

$$0 \leq q_{ct} \leq big M_{gf} b_c \quad (30)$$

$$F_{OC} = \sum_t \left(\sum_g f_g(p_{gt}) + \sum_w Q_w q_{wt} + \sum_s Q_s q_{st} + \right. \quad (31)$$

$$\left. \sum_d Q_d \Delta p_{dt} + \sum_e Q_e \Delta q_{et} \right) \quad (31)$$

$$\Phi_{up} = \{x_l, x_n, x_y, x_c\} \quad (32)$$

$$\Phi_{mid} = \{a_l, a_n, a_y, a_c\} \quad (33)$$

$$\begin{aligned} \Phi_{low} = & \{z_{gt}, z_{nt}, p_{gt}, p_{nt}, \theta_{it}, p_{flt}, p_{mt}, \Delta p_{dt}, \\ & q_{wt}, q_{st}^{in}, q_{st}^{out}, r_{st}, q_{yt}, q_{ct}, v_{jt}, \Delta q_{et}\} \end{aligned} \quad (34)$$

In this formulation, the upper level defense problem consists of (1)-(3). The objective function (1) is to minimize F_{OC} . (2) is the defense budget constraint where X is a positive integer and (3) restricts the decision variables to binary. The middle level attack problem consists of (4)-(6). The objective function (4) is to maximize F_{OC} . Similarly, (5) is the constraint of the attack budget where A is a positive integer and (6) imposes binary restriction on the attack variables. The lower level problem consists of (7)-(30). The objective function (7) is to minimize F_{OC} . (8) represents the operating availability of components after attack, one for normal and zero for failure. (9)-(29) constitute the operating constraints of the gas-electric system. For the electricity network, (9) and (10) enforce the generation capacity of traditional units and gas-fired units, respectively. (11)-(14) are the ramping rate limits of traditional units and gas-fired units, respectively. (15) sets the boundary of not-served load. (16) describes the upper and lower phase angle limits of the power grid. (17) depicts the power balancing condition. (18) is the flow limit for network power. (19) describes the relationship between power flow

and phase angle. For gas systems, (20) limits the production capacity of gas wells. (21) depicts the capacity for gas storage. (22) and (23) impose the range of in and out rate of gas storage, respectively. (24) is the pressure limit of each node. (25) is the gas balance requirement. (26) declares the boundary of the not-served gas load. (27) is the Weymouth equation and it characterizes the relationship between gas flow in a passive pipeline and node pressure. (28) defines the coefficient β_y in the Weymouth equation. (29) implies the pressure relationship between the initial and terminal node of an active pipeline. (30) states the boundary of gas flow in the active pipeline, in which $bigM_{gf}$ is a large enough positive number. In practice, $bigM_{gf}$ can be chosen as the upper bound of the production capacity of the largest gas well. Particularly, the pipelines with and without compressors are referred to as active and passive pipelines, respectively. (31) gives the expression of F_{OC} , in which the first two terms represent the production cost of power and gas, the third term represents the cost of storing gas, the last two terms represent the penalty of not-served power and gas. In (31), $f_g(\cdot)$ might be quadratic and can be further linearized by using the piecewise linear (PWL) approximation method [22]. (32)-(34) define the sets of decision variables for upper, middle and lower level problems, respectively.

Compared with the existing models in [12] and [13] which minimize the sum of not-served power load in a single period, our work reveals the vulnerability information from both economic and security perspectives. To see this, consider the situation that the system is highly flexible or the attack budget is limited, such that there is no load shedding at all. Then no vulnerable components are detected by the existing methods. However, such a flexible response may involve dispatching costly resources in real time. In this regard, we incorporate the production cost of the gas and power load, the operating cost of storage, and the cost of load shedding into the objective function, which allows the operator to protect vulnerable facilities before an attack occurs in a more economical manner.

Another important distinction is considering over-generation of units after the attack, which is neglected in the literature [12], [13], [16]. According to the attacker, a direct attack is to destroy the lines that connect the load with the network. However, an indirect attack, which destroys some lines to cause operation infeasibility even if the generators' output reaches the minimum value in the recourse stage (that is, the recourse action leads generators to an infeasible operating point $P_g^{min}/2$), may cause more catastrophic consequences as some generators have to be cut out, leading to a blackout of the system. From the analysis above, we can see, the unmodeled feature will cause conflict between generator capacity constraint (9)-(10) and nodal power balance constraint (17), leading to a suboptimal attack strategy. Physically, over-generation may trigger a self-protection module and cause a generator outage, leading to an even more catastrophic consequence than the attack itself. To address this issue, the commitment strategy of generators is considered and is controlled by binary variables z_{gt}, z_{nt} in (9)-(14). Its significance is demonstrated in Section IV.C.

B. Linearizing the Weymouth Equation

Clearly, each term in the proposed tri-level formulation is linear except for the gas flow square with sign function in the

Weymouth equation (27), which can be linearized by PWL approximation as follows [19].

$$\psi(q_{yt}) \approx \psi(\Delta_{y1}) + \sum_{k \in K} (\psi(\Delta_{y,k+1}) - \psi(\Delta_{y,k})) \varrho_{ytk} \quad (35)$$

$$q_{yt} = \Delta_{y1} + \sum_{k \in K} (\Delta_{y,k+1} - \Delta_{y,k}) \varrho_{ytk} \quad (36)$$

$$\varrho_{ytk} \leq \zeta_{ytk} \leq \varrho_{ytk}, \forall k \in K - 1 \quad (37)$$

$$0 \leq \varrho_{ytk} \leq 1, \forall k \in K \quad (38)$$

Where Δ_{yk} is the piecewise segment for each passive pipeline and k is the corresponding index; ϱ_{ytk} and ζ_{ytk} are the auxiliary continuous and binary variable, respectively; ψ depicts the relationship between the nonlinear term and gas flow. You can control the error gap of PWL approximation (35)-(38) by choosing the size of K [23].

C. The Compact Model

For ease of analysis, the tri-level D-A-D model in previous subsections can be written in a compact form as follows:

$$Obj_{upper} = \min_{\mathbf{x}} \mathbf{h}^T \mathbf{y} \quad (39)$$

$$s.t. \quad \mathbf{A}\mathbf{x} \leq \mathbf{b} \quad (40)$$

$$Obj_{middle} = \max_{\mathbf{a}} \mathbf{h}^T \mathbf{y} \quad (41)$$

$$s.t. \quad \mathbf{C}\mathbf{a} \leq \mathbf{d} \quad (42)$$

$$Obj_{lower} = \min_{\mathbf{y}, \mathbf{z}} \mathbf{h}^T \mathbf{y} \quad (43)$$

$$s.t. \quad \mathbf{E}(\mathbf{x}, \mathbf{a})\mathbf{y} + \mathbf{F}(\mathbf{x}, \mathbf{a})\mathbf{z} \leq \mathbf{g} \quad (44)$$

Where $\mathbf{x}, \mathbf{a}, \mathbf{z}$ are binary variable vectors, \mathbf{y} is a continuous variable vector, and $\mathbf{A}, \mathbf{C}, \mathbf{b}, \mathbf{d}, \mathbf{g}$, and \mathbf{h} are constant coefficient matrices which can be derived from (2), (5), and (9)-(30). Specifically, $\mathbf{E}(\mathbf{x}, \mathbf{a})$ and $\mathbf{F}(\mathbf{x}, \mathbf{a})$ are variable coefficient matrices and can be derived from (9)-(30). It is worth mentioning that in its current formulation, we consider only the redispatch cost $\mathbf{h}^T \mathbf{y}$ in the objective function, however, there is no difficulty if one prefers to use a more general cost function in the form of $\mathbf{h}_1^T \mathbf{x} + \mathbf{h}_2^T \mathbf{z} + \mathbf{h}_3^T \mathbf{y}$.

III. SOLUTION METHODOLOGY

In general, several decomposition methods are available to solve a linear min-max-min model such as Benders decomposition [24], [25] and column and constraint generation (C&CG) [18]. However, the presence of binary variables prevents directly dualizing the lower level problem. We adopt a nested C&CG method in [20] to solve the D-A-D problem (39)-(44). The application of the nested C&CG method has been found in the robust unit commitment with quick-start units [17], which shows its potential for the proposed formulation.

A. Inner C&CG for Middle Lower-Level Problem

With fixed defense strategy \mathbf{x}^* and lower-level binary variable \mathbf{z}^* , (44) yields the following inequality

$$\mathbf{E}(\mathbf{x}^*, \mathbf{a})\mathbf{y} \leq \mathbf{g} - \mathbf{F}(\mathbf{x}^*, \mathbf{a})\mathbf{z}^* \quad (45)$$

Then the linear program consisting of (43) and (45) with $\mathbf{z} = \mathbf{z}^*$ can be replaced by its dual form as follows

$$\max_{\mu} (g - F(x^*, a)z^*)^T \mu \quad (46)$$

$$s.t. E(x^*, a)^T \mu = h, \mu \leq 0 \quad (47)$$

Where μ is the dual variable. The middle lower-level problem (41)-(44) can be solved by the *C&CG* algorithm described below, denoted as *Algo_{inner}*.

Step 1: Select an arbitrary feasible attack strategy a^* , and solve the following problem:

$$\min_{y, z} h^T y \quad (48)$$

$$s.t. E(x^*, a^*)y + F(x^*, a^*)z \leq g$$

Denote the optimal solution by y^*, z^* , set $LB = h^T y^*$, $UB = +\infty$, $o = 1$, $z^{1*} = z^*$, $O = \{1\}$, $Z = \{z^{1*}\}$.

Step 2: Solve the following problem

$$Obj_{middle} = \max_{\theta, a, \mu} \theta \quad (49)$$

$$s.t. \theta \leq (g - F(x^*, a)z^{r*})^T \mu^r, \forall r \in O, z^{r*} \in Z \quad (50)$$

$$Ca \leq d, E(x^*, a)^T \mu^r \leq h^T, \mu^r \leq 0, \forall r \in O \quad (51)$$

Extract the optimal solution a^* and θ^* , and update $UB = \theta^*$.

Step 3: Solve (48) with a^* , obtain the optimal solution (z^*, y^*) and update $LB = \max\{LB, h^T y^*\}$.

Step 4: If $UB - LB \leq \epsilon$, terminate and, return the attack strategy a^* and the optimal value Obj_{middle}^* . Otherwise, update $o = o + 1$, $O = O \cup o + 1$, $z^{o*} = z^*$, $Z = Z \cup z^{o*}$, create new variables μ^o with the following constraints,

$$\theta \leq (g - F(x^*, a)z^{o*})^T \mu^o \quad (52)$$

$$E(x^*, a)^T \mu^o \leq h^T, \mu^o \leq 0 \quad (53)$$

and go to Step 2.

Note that there are bilinear terms in (50) and (51) which can be further linearized, and Section III.C discusses them. Then problem (49)-(51) can be reformulated as a MILP, which is readily solvable by commercial software. By calling *Algo_{inner}*, the optimal attack strategy a^* under fixed defense strategy x^* can be obtained.

B. Outer C&CG for Upper Level Problem

The outer *C&CG* algorithm for the upper level problem, denoted as *Algo_{outer}*, identifies the optimal defense strategy under all possible attacks, which proceeds as follows.

Step 1: Set $LB = -\infty$, $UB = +\infty$, $a^{1*} = 0$, $w = 1$, $W = \{w\}$, and select a convergence tolerant ϵ_{outer} .

Step 2: Solve the following problem:

$$Obj_{upper} = \min_{x, y, z} \varphi \quad (54)$$

$$s.t. Ax \leq b, \varphi \leq h^T y^f, \forall f \in W \quad (55)$$

$$E(x, a^{f*})y^f + F(x, a^{f*})z^f \leq g, \forall f \in W \quad (56)$$

Let the optimal solution be x^* , the optimal value φ^* , and update $LB = \min(UB, \varphi^*)$.

Step 3: Call *Algo_{inner}*, obtain the optimal solution a^* and optimal value Obj_{middle}^* , update $UB = \min(UB, Obj_{middle}^*)$.

Step 4: If $UB - LB \leq \epsilon_{outer}$, terminate and return the optimal solution x^*, a^*, y^*, z^* . Otherwise, update $w = w + 1$, $W = W \cup w$, $a^{w*} = a^*$, create new variables (y^w, z^w) with the following constraints, and go to Step 2.

$$\varphi \leq h^T y^w \quad (57)$$

$$E(x, a^{w*})y^w + F(x, a^{w*})z^w \leq g \quad (58)$$

Similarly, there are bilinear terms in (56) which can be further linearized, and the next subsection discusses them. Then the problem in Step 2 can be transformed into a MILP.

C. Linearization of Bilinear Terms

The bilinear terms in *Algo_{inner}* and *Algo_{outer}* include binary production and binary-continuous production. The corresponding linearization methods are shown below.

1) *Binary production:* The binary production terms exist in (10), namely $F(x, a^*)z^r$ of (56). Take $\delta = \kappa\lambda$ for example, where κ and λ are binary, and their multiplication δ is another binary variable. It is easy to verify that above equality is equivalent to the following linear constraints

$$\kappa + \lambda - \delta - 1 \leq 0 \quad (59)$$

$$\delta - \kappa \leq 0 \quad (60)$$

$$\delta - \lambda \leq 0 \quad (61)$$

2) *Binary-continuous production:* The binary-continuous production terms exist in (19), (27), (29), namely $E(x, a^*)y^r$ of (56). Again, take $\delta = \kappa\lambda$ for example, where κ is binary and λ is continuous. Their multiplication δ is a continuous variable. It is easy to verify that above equality is equivalent to the following linear constraints

$$\lambda^{min} \kappa \leq \delta \leq \lambda^{max} \kappa \quad (62)$$

$$\lambda^{min}(1 - \kappa) \leq \lambda - \delta \leq \lambda^{max}(1 - \kappa) \quad (63)$$

where λ^{min} and λ^{max} are the lower bound and upper bound of λ , respectively. If they are not known precisely, we can use a large constant $BigM_{con}$ instead. In practice, choosing the value of $BigM_{con}$ can be tricky: if $BigM_{con}$ is too large, the continuous relaxation of the MILP will be rather weak, this will cause unnecessary computational burden in the branch and bound procedure; on the other hand, if $BigM_{con}$ is too small, there will be a duality gap between problem (46)-(47) and its primal problem, and the reformulation will be incorrect. Due to the physical operating constraints, the bounds of primal variables (say the gas pressure and the power transmission line capacity) are easy to retrieve, and the bounds of dual variables are not instantly apparent.

To reduce the proper value of $BigM_{con}$, the objective function (31) is divided by an auxiliary parameter $BigM_{obj}$. A heuristic choice of $BigM_{obj}$ may be the objective value when all loads are not-served. To see this, consider the following primal-dual pair of LPs:

$$P: \min \{c^T x \mid Ax \leq b\}$$

$$D: \max \{b^T y \mid A^T y = c, y \leq 0\}$$

Due to physical operation constraints, the feasible region of problem P is a bounded polytope, and a finite optimal value $c^T x^*$ can be found at one of its extreme points x^* . According

to the duality theory of LP, problem D must have a finite optimal value $b^T y^* = c^T x^*$ with bounded y^* , although the feasible region of D may be unbounded. In transformation (62) and (63), the $BigM_{con}$ parameter of the dual variable should satisfy $-BigM_{con} \leq y^*$ such that the optimal solution is not influenced. The difficulty lies in the fact that y^* is not known in advance, so we have to use a large enough value, which might be overly pessimistic. However, if the objective of P becomes $c^T x / BigM_{obj}$, the optimal solution x^* of problem P remains the same, and it is easy to verify that $y = y^* / BigM_{obj}$ is an optimal solution of problem D. This indicates that the bound parameter $BigM_{con}$ imposed on the dual variables can be reduced. Section IV.D shows the numeric results.

IV. ILLUSTRATIVE EXAMPLE

In this section, we present numerical experiments on two test systems to show the effectiveness of the proposed model and algorithm. The experiments are performed on a laptop with Intel(R) Core(TM) 2 Duo 2.2 GHz CPU and 4 GB memory. The proposed algorithms are implemented on MATLAB with YALMIP toolbox. MILP is solved by Gurobi 6.5, the optimality gap is set as 0.1% without particular mention.

A. 6-Bus Power System with 7-Node Gas System

Fig. 1 depicts the topology of the connected infrastructure. It has 2 gas-fired units, 1 traditional unit, 2 gas wells, 1 compressor, 1 gas storage tank, 3 power loads and 3 gas loads. The targets of the attacker are the 7 power transmission lines, 5 passive pipelines, 1 active pipeline and 2 connection lines. Here the connection lines represent the gas pipelines that transport gas to gas-fired units. The parameters of the system and the scheduled unit commitment can be found in [26]. In the following cases, we consider the problem with $T = 4$ periods. The power and gas demand profiles are shown in Fig. 2, in which four typical time slots are selected. Details of these time slots are shown in Table I. We set $K = 8$ in (35)-(38), which means that an eight-segment linear approximation replaces the nonlinear Weymouth equation.

TABLE I
DETAILS OF THE SELECTED TIME SLOTS

Case	Periods	Power	Gas
1	2-5	low	low
2	9-12	mid	mid
3	14-17	high	mid
4	19-22	mid	high

B. Computational Results

In this subsection, $X = 3$ and $A = 3$ are selected as the benchmark and the corresponding results are summarized in Table II, where *Def*, *Atk*, *OC*, *NP*, *NG* are short for *Defend Resource*, *Attack Resource*, *Operational Cost*, *Not-served Power* and *Not-served Gas*, respectively. As the gas system is radial and the power system is meshed in topology, the production resources of the gas system are more centralized than the power system and more vulnerable to attacks. Thus the defense resources are spent mainly on the gas system.

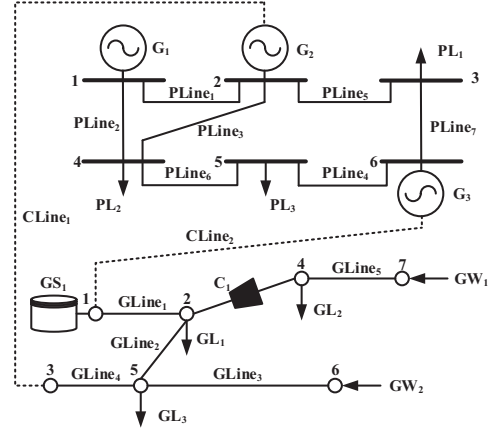


Fig. 1. Topology of the hybrid test system.

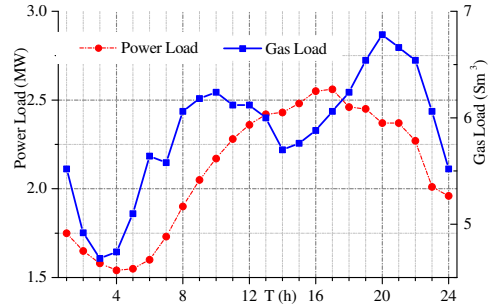


Fig. 2. Power and gas demand.

Similar circumstance occurs in the attacker's strategy. The attack priority is the gas system unless the gas load is in low level, that is, case 1. The average power and gas loss rates of the four time plots under the optimal attack strategy are 48.6% and 6.55%, respectively, assuming the optimal deployment of defense resources. This difference reveals that the failure of the gas system will have a larger impact on the coupled physical system, as the energy from gas system to power system is a one-way flow. Also, we consider both the defense and attack budget variables, whose range varies in the intervals $[1, N + L + C + Y - 1]$ and $[1, N + L + C + Y - A]$, respectively. Various tests are carried out under different defense budgets, attack budgets, and time slots. Fig. 3 shows the results. Here we define the defense rate of a component as the number of instances in which it is protected divided by the total number of defense and attack budget combinations, for example, $GLine_5$ is defended in 99 out of 105 defense and attack budget combinations in case 3, thus its defense rate is 94.26%, as shown in Fig. 3. The importance of each component is seen by the relative value of the defense rate in Fig. 3, from which we can observe $GLine_5$ is always the most important component, as its defense rate is the highest in all cases. Also, the defense rate of a specific component varies from case to case, which reveals that the defense strategy depends on the load level.

To demonstrate the benefit of prior protection, the operation cost under different combinations of defense and attack budget are shown in Fig. 4. from which we can see, with defense budget increasing, the average operation cost under

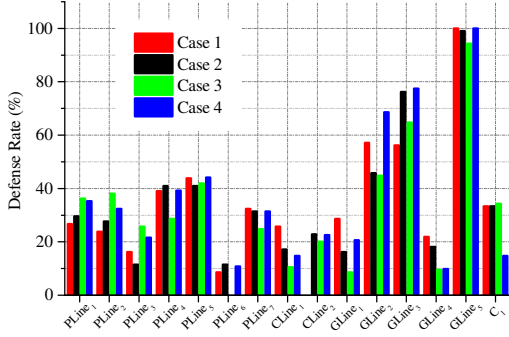


Fig. 3. Defense rate of components under 4 cases.

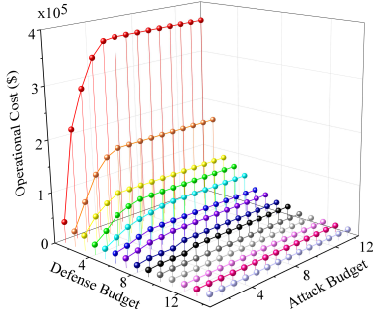


Fig. 4. Operational cost under different budgets.

different attack budgets decreases. However, the decrement of operational cost also decreases. Specifically, when the defense budget is 8 or larger, the attack budget has little impact on the operation cost. Moreover, if the attack budget is limited, the operation cost can be well-controlled through a limited defense budget, say $X = 4$ in this case, which may provide guidance for defense budgeting.

TABLE II
COMPUTATIONAL RESULTS UNDER THE BENCHMARK

Case	Def	Atk	OC(\$)	NP (MWh)	NG (Sm^3)
1	$GLine_2$	$GLine_1$	6.713×10^5	664	0
	$GLine_3$	$GLine_4$			
	$GLine_5$	$PLine_5$			
2	C_1	$PLine_2$	7.529×10^5	310	2261
	$GLine_3$	$PLine_3$			
	$GLine_5$	$PLine_4$			
3	C_1	$CLine_1$	8.615×10^5	0	3900
	$GLine_5$	$PLine_1$			
	$PLine_5$	$PLine_2$			
4	C_1	$PLine_2$	8.047×10^5	795	0
	$GLine_3$	$PLine_3$			
	$GLine_5$	$PLine_4$			

C. Significance of Considering Over-generation

This subsection discussed the significance of incorporating over-generation. To make the result clear, we assume only power transmission lines can be attacked in the tests. We set $X = 2$ and $A = 2$, and list the corresponding results in Table III. These results shown that, the sum of the attack

strategy is smaller than the attack budget in cases 1-4 if over-generation is not considered, which indicates that any additional attack will cause over-generation and will not be allowed. Further, the optimal defense strategy with or without over-generation attack (OGA) is also quite different, which confirms the need to consider over-generation when deploying corrective actions.

TABLE III
COMPUTATIONAL RESULT WITHOUT OVER-GENERATION ATTACK

Case	Def	Atk	OC(\$)	NP (MWh)	
1	OGA	$PLine_5$ $PLine_7$	$PLine_1$ $PLine_3$	2.764×10^5	56.1
	no OGA	$PLine_3$ $PLine_4$	$PLine_1$	2.201×10^5	0
2	OGA	$PLine_1$ $PLine_2$	$PLine_4$ $PLine_5$	3.469×10^5	49.6
	no OGA	$PLine_2$ $PLine_4$	$PLine_1$	2.969×10^5	0
3	OGA	$PLine_2$ $PLine_3$	$PLine_5$ $PLine_6$	4.405×10^5	432
	no OGA	$PLine_3$ $PLine_4$	$PLine_1$	2.827×10^5	55.8
4	OGA	$PLine_2$ $PLine_6$	$PLine_3$ $PLine_4$	4.027×10^5	394
	no OGA	$PLine_2$ $PLine_4$	$PLine_1$	2.194×10^5	7.25

D. Impact of $BigM_{obj}$

As mentioned in section III.C, the value of $BigM_{con}$ for unbounded dual variables will significantly impact the computational efficiency. Different from [12] and [13], Fig. 5 shows the active lower bound of $BigM_{con}$ as well as computational time along with the variation of $BigM_{obj}$. This shows, the active lower bound of the magnitude of $BigM_{con}$ keeps decreasing as $BigM_{obj}$ decreases, which confirms the analysis in section III.C. However, the computational time is non-monotonic with respect to $BigM_{obj}$. The reason may be that, at the very beginning, as $BigM_{obj}$ decreases, the range of $BigM_{con}$ shrinks, which would lead to a stronger MILP formulation and thus reduce the computational burden; however, as $BigM_{obj}$ keeps decreasing, the range of $BigM_{con}$ may become too small and step out of the numerical stability range, leading in turn to an ill-conditioned problem. Nevertheless, $BigM_{obj}$ has a relatively wide ideal range from the aspect of computational efficiency, which is $[10^4, 10^6]$ in this case, as Fig. 5 indicates, demonstrating the promising prospect of practical application for the proposed method.

E. 39-Bus Power System with 20-Node Gas Network

In this subsection, we apply the proposed model and algorithm to a larger test system, which comprises the IEEE 39-bus system and a modified version of the Belgian high-calorific 20-node gas network. It has 3 gas-fired units, 7 traditional units, 2 gas wells, 3 compressors, 4 gas storage tanks, 19 power loads and 9 gas loads. Similar to the settings in section IV. A, all the system branches are the targets of the attacker, including 46 power transmission lines, 21 passive pipelines, 3 active pipelines and 3 connection lines. Refer to [26] for

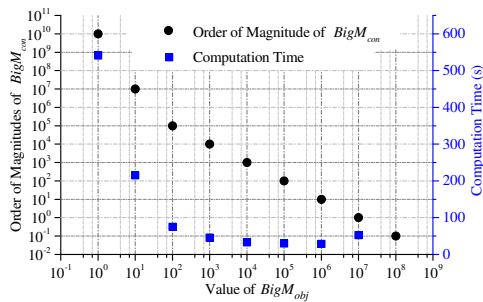


Fig. 5. Value of $BigM$ and computation time.

the topology, parameters, and unit commitment of the test system as well as the power and gas demand. We consider $T = 2$ periods and $K = 4$ for the Weymouth equation approximation and a 1% optimality gap as a trade-off between solution accuracy and computational burden. We select period 2 to 3, 9 to 10, 14 to 15 and 19 to 20, as four target time slots. Table IV summarizes the average computation time under different combinations of defense and attack budget. The results show that the computation time increases rapidly as the defense and attack budget increase. However, when the defense and attack budget are limited, the computation time is acceptable, demonstrating the scalability of the proposed model and algorithm to moderately sized systems.

TABLE IV
COMPUTATION TIME (S) UNDER DIFFERENT BUDGETS

Atk \ Def	1	2	3	4	5
1	65	77	93	111	140
2	155	172	312	551	673
3	317	477	699	831	1145
4	663	927	1401	2022	2712
5	922	1477	1902	2638	3531

V. CONCLUSION

The proposed methodology addresses the vulnerability of coupled gas-electric networks against malicious line interdictions. It provides the optimal strategies for preventive reinforcement, and increases the resilience of the energy supply, and decreases the operational cost of the interdependent energy systems. The mixed integer linear representation of the over-generation issue and the gas system constraints entails binary variables in the lower level problem, and prevents a traditional C&CG algorithm being applied. A nested C&CG algorithm is adopted and the corresponding computational burden is reduced by choosing the proper value of $BigM_{con}$, which enhances the applicability of the proposed method. Simulation results corroborate the effectiveness of the proposed method, and suggest giving higher priority to protecting systems with radial topology.

REFERENCES

[1] M. Shahidehpour, Y. Fu, and T. Wiedman, "Impact of natural gas infrastructure on electric power systems," *Proc. of the IEEE*, vol. 93, no. 5, pp. 1042–1056, May 2005.

[2] C. Liu, M. Shahidehpour, Y. Fu, and Z. Li, "Security-constrained unit commitment with natural gas transmission constraints," *IEEE Trans. Power Syst.*, vol. 24, no. 3, pp. 1523–1536, Aug. 2009.

[3] X. Zhang, M. Shahidehpour, A. S. Alabdulwahab, and A. Abusorrah, "Security-constrained co-optimization planning of electricity and natural gas transportation infrastructures," *IEEE Trans. Power Syst.*, vol. 30, no. 6, pp. 2984–2993, Nov. 2015.

[4] C. M. Correa-Posada and P. Sánchez-Martín, "Security-constrained optimal power and natural-gas flow," *IEEE Trans. Power Syst.*, vol. 29, no. 4, pp. 1780–1787, Jul. 2014.

[5] A. Alabdulwahab, A. Abusorrah, X. Zhang, and M. Shahidehpour, "Coordination of interdependent natural gas and electricity infrastructures for firming the variability of wind energy in stochastic day-ahead scheduling," *IEEE Trans. Sustain Energy*, vol. 6, no. 2, pp. 606–615, Apr. 2015.

[6] C. Liu, C. Lee, and M. Shahidehpour, "Look ahead robust scheduling of wind-thermal system with considering natural gas congestion," *IEEE Trans. Power Syst.*, vol. 30, no. 1, pp. 544–545, Jan. 2015.

[7] J. Devlin, K. Li, P. Higgins, and A. Foley, "The importance of gas infrastructure in power systems with high wind power penetrations," *Appl. Energy*, vol. PP, no. 99, pp. 1–11.

[8] M. Bailera, P. Lisb, L. M. Romeo, and S. Espotolero, "Power to gas-biomass oxycombustion hybrid system: energy integration and potential applications," *Appl. Energy*, vol. PP, no. 99, pp. 1–9.

[9] M. Qadrdan, M. Abeysekera, M. Chaudry, J. Wu, and N. Jenkins, "Role of power-to-gas in an integrated gas and electricity system in Great Britain," *Int. J. Hydrogen Energy*, vol. 50, no. 17, pp. 5763–5775, 2015.

[10] J. Salmeron, K. Wood, and R. Baldick, "Analysis of electric grid security under terrorist threat," *IEEE Trans. Power Syst.*, vol. 19, no. 2, pp. 905–912, May 2004.

[11] —, "Worst-case interdiction analysis of large-scale electric power grids," *IEEE Trans. Power Syst.*, vol. 24, no. 1, pp. 96–104, Feb. 2009.

[12] J. M. Arroyo, "Bilevel programming applied to power system vulnerability analysis under multiple contingencies," *IET Gener. Transm. Distrib.*, vol. 4, no. 2, pp. 178–190, Feb. 2010.

[13] Y. Wei, L. Zhao, and B. Zeng, "Optimal power grid protection through a defender-attacker-defender model," *Reliab. Eng. Syst. Safe.*, vol. 121, pp. 83–89, Jan. 2014.

[14] N. Alguacil, A. Delgado, and J. Arroyo, "A trilevel programming approach for electric grid defense planning," *Comp. & Oper. Res.*, vol. 41, pp. 282–290, Jan. 2014.

[15] R. Carvalho, L. Buzna, F. Bono, M. Masera, D. Arrowsmith, and D. Helbing, "Resilience of natural gas networks during conflicts, crises and disruptions," *PLoS One*, vol. 9, no. 3, pp. 1–9, Mar. 2014.

[16] S. Manshadi and M. Khodayar, "Resilient operation of multiple energy carrier microgrids," *IEEE Trans. Smart Grid*, vol. 6, no. 5, pp. 2283–2292, Sep. 2015.

[17] B. Hu and L. Wu., "Robust SCUC considering continuous/discrete uncertainties and quick-start units: A two-stage robust optimization with mixed-integer recourse," *IEEE Trans. Power Syst.*, vol. 31, no. 2, pp. 1407–1419, Mar. 2016.

[18] B. Zeng and L. Zhao, "Solving two-stage robust optimization using a column-and-constraint generation method," *Oper. Res. Lett.*, vol. 41, no. 5, pp. 457–461, Sep. 2013.

[19] C. Correa-Posada and P. Sanchez-Martín, "Integrated power and natural gas model for energy adequacy in short-term operation," *IEEE Trans. Power Syst.*, vol. 30, no. 6, pp. 3347–3355, Nov. 2015.

[20] L. Zhao and B. Zeng. (2012) An exact algorithm for two-stage robust optimization with mixed integer recourse problems. [Online]. Available: http://www.optimization-online.org/DB_FILE/2012/01/3310.pdf

[21] D. Wolf and Y. Smeers, "The gas transmission problem solved by an extension of the simplex algorithm," *Manage. Sci.*, vol. 46, no. 11, pp. 1454–1465, Nov. 2000.

[22] M. Carrion and J. M. Arroyo, "A computationally efficient mixed-integer linear formulation for the thermal unit commitment problem," *IEEE Trans. Power Syst.*, vol. 21, no. 3, pp. 1371–1378, Aug. 2006.

[23] C. Correa-Posada and P. Sanchez-Martín. (2014) Gas network optimization: A comparison of piecewise linear models. [Online]. Available: http://www.optimization-online.org/DB_FILE/2014/10/4580.pdf

[24] A. Geoffrion, "Generalized benders decomposition," *J. Optim. Theory Appl.*, vol. 10, no. 4, pp. 237–260, Oct. 1972.

[25] D. Bertsimas, E. Litvinov, X. A. Sun, J. Zhao, and T. Zheng, "Adaptive robust optimization for the security constrained unit commitment problem," *IEEE Trans. Power Syst.*, vol. 28, no. 1, pp. 52–63, Feb. 2013.

[26] [Online]. Available: <https://sites.google.com/site/chengwang0617/home/data-sheet>